

# Reactive Oxygen Species Control Osteoblast Apoptosis through SIRT1/PGC-1 $\alpha$ /P53<sup>Lys382</sup> Signaling, Mediating the Onset of Cd-Induced Osteoporosis

Published as part of the Journal of Agricultural and Food Chemistry *virtual special issue* “The Future of Agriculture and Food: Sustainable Approaches to Achieve Zero Hunger”.

Di Ran, Dehui Zhou, Gang Liu, Yonggang Ma, Waseem Ali, Rui Yu, Qinghua Wang, Hongyan Zhao, Jiaqiao Zhu, Hui Zou,<sup>\*, $\perp$</sup>  and Zongping Liu<sup>\*, $\perp$</sup>



Cite This: *J. Agric. Food Chem.* 2023, 71, 5991–6002



Read Online

ACCESS |

Metrics & More

Article Recommendations

**ABSTRACT:** The imbalance between osteogenesis and osteoclastogenesis is a feature of bone metabolic disease. Cadmium (Cd) exposure causes human bone loss and osteoporosis (OP) through bioaccumulation of the food chain. However, the impact of Cd on bone tissues and the underlying molecular mechanisms are not well-characterized. In the current study, we found that the Cd concentration in bone tissues of OP patients was higher than normal subjects; meanwhile, the nuclear silent information regulator of transcription 1 (SIRT1) protein expression level was significantly decreased, which is a new star molecule to treat OP. It is further revealed that SIRT1 activation markedly reprograms bone metabolic and stress-response pathways that incline with osteoblast (OB) apoptosis. Suppressing reactive oxygen species (ROS) release with *N*-acetyl-L-cysteine (NAC) abolished Cd-induced reduction of SIRT1 protein, deacetylation of P53, OB apoptosis, and attenuated OP. Conversely, overexpression of SIRT1 suppressed Cd-induced ROS release. SIRT1 overexpression *in vivo* and *in vitro* dampened PGC-1 $\alpha$  protein, acetylation of P53 at lysine 382, and caspase-dependent apoptosis. These results reveal that ROS/SIRT1 controls P53 acetylation and coordinates OB apoptosis involved in the onset of OP.

**KEYWORDS:** cadmium, osteoporosis, osteoblast, ROS, apoptosis

## INTRODUCTION

Cadmium (Cd) is one of the most toxic trace elements that causes bone disorders, including osteopenia and osteoporosis (OP).<sup>1</sup> Cd accumulation in human tissues shows significant variations among individuals and is highly associated with bone fracture, cancer, kidney dysfunction, and hypertension.<sup>2</sup> Despite this, the precise mechanisms of Cd-exposure-induced bone metabolism disorders remain elusive. Although some previous studies have suggested Cd toxicity to bone tissues as a result of kidney damage, which may result from defects in nutrition absorption and vitamin D metabolism,<sup>3</sup> a growing body of evidence indicates that Cd exposure directly affects osteogenesis independent of nephrotoxicity.<sup>4</sup> The concentration and exposure duration of Cd are the main factors influencing bone injury. Short-term (4 months) CdCl<sub>2</sub> exposure (25 mg/L) has no apparent effects on mice bone tissues. However, long-term (15 months) CdCl<sub>2</sub> exposure (25 mg/L) decreased the bone mineral density (BMD) value and promoted the procession of OP.<sup>5</sup> Yang et al. found that 50 mg/L CdCl<sub>2</sub> exposure for 3 months could induce OP in mice.<sup>6</sup> Furthermore, different species show various sensitivities to Cd. The previous studies found that 1  $\mu$ M CdCl<sub>2</sub> exposure for 14 days causes OP in ducks. Similarly 2–20  $\mu$ M CdCl<sub>2</sub> decreased bone formation in chick embryonic long bones *in vitro*.<sup>7</sup>

Moreover, urine cadmium concentrations were up to 20–30  $\mu$ g of Cd/g of creatinine.<sup>8</sup> OP and osteoporotic fractures have become a major public health concern globally and a massive socioeconomic burden.<sup>9</sup>

The imbalance in bone formation by osteoblasts and resorption by osteoclasts plays a key role in bone homeostasis, leading to bone loss, which is implicated in the pathogenesis of OP. OP is characterized by bone microarchitecture deterioration and low BMD.<sup>10</sup> Silent information regulator of transcription 1 (SIRT1) participates in diverse cellular processes and plays a critical role in normal skeletal development and homeostasis. Cheng et al. investigated developmental defects and P53 hyperacetylation in SIRT1-deficient mice. They found that, in comparison to wild-type control mice, SIRT1-deficient mice were at a low healthy score and low survival rate postnatally.<sup>11</sup> Moreover, mutant mice showed craniofacial abnormalities, including defects in the

**Received:** December 3, 2022

**Revised:** March 21, 2023

**Accepted:** March 29, 2023

**Published:** April 6, 2023

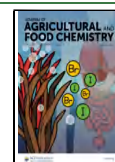


Table 1. List of Six Normal Individuals and Six Individuals with OP in This Study

	normal					OP						
	M	M	F	M	F	M	F	M	F	F	F	F
gender												
age (year)	68.9	62.6	58.1	69.5	58.4	57.2	62.1	57.6	55.3	65.2	58	52.2
BMD (g/cm <sup>2</sup> )	1.187	1.34	1.52	1.052	0.998	1.062	0.625	0.823	0.852	0.55	0.71	0.68

development and closure of craniofacial sutures, abnormal palate architecture, and exencephaly.<sup>11,12</sup> Cohen et al. found that hormone and endocrine signaling pathways were related to SIRT1 via bone remodeling.<sup>13</sup> Ovariectomized (OVX) mice reportedly show downregulated SIRT1 expression, and resveratrol protects against bone loss in OVX models of postmenopausal OP by SIRT1 activation.<sup>14</sup> These studies hint at the key function of SIRT1 in bone homeostasis.

Mitochondrial dysfunction,<sup>15</sup> oxidative stress,<sup>16</sup> and DNA damage response (DDR)<sup>17</sup> are closely related to cellular homeostasis impairment and contribute to OP progression. Mitochondria supply adenosine triphosphate (ATP), which is necessary for survival, and mitochondrial dysfunction is reportedly associated with OP.<sup>18</sup> SIRT1 improves mitochondrial health and is therefore essential for regulating reactive oxygen species (ROS) levels and mitochondrial biogenesis.<sup>19</sup> ROS-induced DNA damage and cellular apoptosis are responsible for tissue dysfunction and bone homeostasis imbalance.<sup>20</sup> Accordingly, targeting the maintenance of mitochondrial quality through SIRT1 appears to be a promising therapeutic approach for OP. The objective of the current study was to evaluate the effects of CdCl<sub>2</sub> exposure on bone tissue damage in rats and humans. Moreover, we also aim to test whether SIRT1 is involved in CdCl<sub>2</sub>-induced bone injury *in vivo* and *in vitro*, to demonstrate SIRT1 in OP and identify an effective therapeutic target for OP.

## MATERIALS AND METHODS

**Chemicals.** N-Acetyl-L-cysteine (NAC) and cadmium chloride (CdCl<sub>2</sub>) were obtained from Sigma Chemicals. The antibodies of SIRT1, cleaved caspase 9, cleaved caspase 3, Bcl-2-associated X (Bax), and Bcl-2 were purchased from Cell Signaling Technology (CST, Boston, MA, U.S.A.). Histone H3 and  $\beta$ -actin were purchased from Abclonal. The antibody diluent was purchased from NCM. The bicinchoninic acid (BCA) kit was purchased from Yeasen (Shanghai, China).

**Experimental Animals.** Adult female Sprague Dawley rats ( $n = 50$ , 4 weeks old,  $120 \pm 5$  g) were approved for use by the Animal Care and Use Committee of Yangzhou University (approval ID SYXK [Su] 2007-0005). They were housed in a controlled environment under automatically well-controlled conditions ( $23 \pm 1$  °C, 12/12 h, and light/dark cycle) for 1 week. A total of 10 OVX rats comprised the OP group and were used to establish the OVX rat model of OP successfully; a total of 10 rats comprised the sham operation group; and other rats were randomly assigned to the CdCl<sub>2</sub>-treated, NAC and CdCl<sub>2</sub> co-treated, and AAV-SIRT1 and CdCl<sub>2</sub>-treated groups ( $n = 10$ /group).

The animals were treated with NAC (0.4 mg/L) and CdCl<sub>2</sub> (50 mg/L) (Sigma-Aldrich, St. Louis, MO, U.S.A.) dissolved in double-deionized water. All treatments were administered as a single daily dose for 18 consecutive months. AAV-ePHB-*ove*-SIRT1 viruses were purchased from Hanheng Biotechnology Co., Ltd. The rats were anesthetized with an intraperitoneal injection of 80–100 mg/kg of pentobarbital sodium, and the virus was injected through the caudal vein. The CdCl<sub>2</sub> dose was the same as that used in previous studies;<sup>6</sup> at this dose, CdCl<sub>2</sub> has apparent effects on bone tissues, with neural damage mainly occurring via oxidative stress activation. The NAC dose was as per that reported by another study based on a different animal model.<sup>21</sup> Considering that the “itai-itai disease” mostly occurs

in women, in this study, only female Sprague Dawley rats were included.

**Ethics.** The institutional ethics review board approved this study, with the collection of bone tissues from six normal individuals and six individuals with OP (the information shown in Table 1) living in North Jiangsu Province in China.

**Cell Culture, Transfection, and Treatment.** The rat osteoblast cell line ROS1728 was purchased from the American Tissue Culture Collection (Manassas, VA, U.S.A.). Cells were suspended in Dulbecco's modified Eagle's medium containing 10% fetal bovine serum (2 mM L-glutamine, 100 units/mL penicillin, and 100  $\mu$ g/mL streptomycin). Lentivirus-mediated SIRT1 shRNA was constructed by ViGene Biosciences (Shandong, China), and scramble shRNA acted as the blank control. Approximately 10 000 osteoblasts were cultured in six-well plates, followed by the addition of lentivirus-mediated SIRT1 shRNA and incubation for 48 h. Cells were treated with concentrations of CdCl<sub>2</sub> (0–80  $\mu$ M) for 6 h. In some experiments, cells were pretreated with NAC (10  $\mu$ M) for 1 h or transfected with lentivirus-mediated SIRT1 shRNA for 48 h before exposure to 40  $\mu$ M CdCl<sub>2</sub>.

**Transmission Electron Microscopy (TEM).** Osteoblasts were fixed in modified Karnovsky's fixative for 12 h, and the bone tissue of rats and humans was cut into 1 mm<sup>3</sup> squares, washed twice with phosphate-buffered saline (PBS), and fixed in modified Karnovsky's fixative for 24 h, with the treatment of 1% osmium tetroxide in 0.1 M cacodylate buffer for 1 h. Next, 1% uranyl acetate was used to strain and dehydrated in ethanol. Epoxy resin was used to embed cells (sectioned 60–70 nm), placed on Formvar- and carbon-coated copper grids, and finally strained with uranyl acetate and lead nitrate. Images were captured with a JEOL 1200EX II transmission electron microscope.

**Western Blotting.** Simply, as in previous studies, osteoblasts were treated with CdCl<sub>2</sub> (0, 20, 40, and 80  $\mu$ M) for 6 h or were pretreated with NAC (10  $\mu$ M) for 1 h and then treated with 40  $\mu$ M CdCl<sub>2</sub> for 6 h. Nuclear proteins and total proteins were extracted and qualified. Equivative proteins were separated with dodecyl sulfate polyacrylamide gels and transferred to polyvinylidene fluoride membranes (Millipore, Danvers, MA, U.S.A.). A 5% skim milk was used to block the membrane for 2 h and incubate the relative primary and secondary antibodies. Images were captured with chemiluminescence (NCM).<sup>22</sup>

**Antioxidant Ability Detection.** Intracellular ROS levels in osteoblasts were detected with 2',7'-dichlorofluorescein diacetate (DCFH-DA, Yeasen, Shanghai, China) according to the instructions of the manufacturer. Intracellular ROS, superoxide dismutase (SOD), and malondialdehyde (MDA) levels in the serum were detected using rat intracellular ROS, SOD, and MDA enzyme-linked immunosorbent assay (ELISA) kits, respectively (MLBio, Shanghai, China).

**Measurement of Apoptosis Rates of Osteoblasts by Flow Cytometry.** The rate of cell apoptosis was assayed using the Annexin V<sup>+</sup>/fluorescein isothiocyanate (FITC) apoptosis kit (Vazyme, Shanghai, China). Briefly, the cells were stained by Annexin V<sup>+</sup> and propidium iodide (PI) for 30 min at 37 °C in the dark, washed with PBS twice, then resuspended, and finally analyzed using flow cytometry (BD, Franklin Lakes, NJ, U.S.A.).

**Histopathological Assessment.** Hematoxylin and eosin (H&E) staining was carried out with standard methods.<sup>6</sup> Briefly, the bone tissues were decalcified with Perenyi's solution for 2 weeks and then an ethanol gradient (75, 90, and 100%) used to dehydrate and embedded in paraffin. They were sectioned with a microtome at 5–8  $\mu$ m thickness.

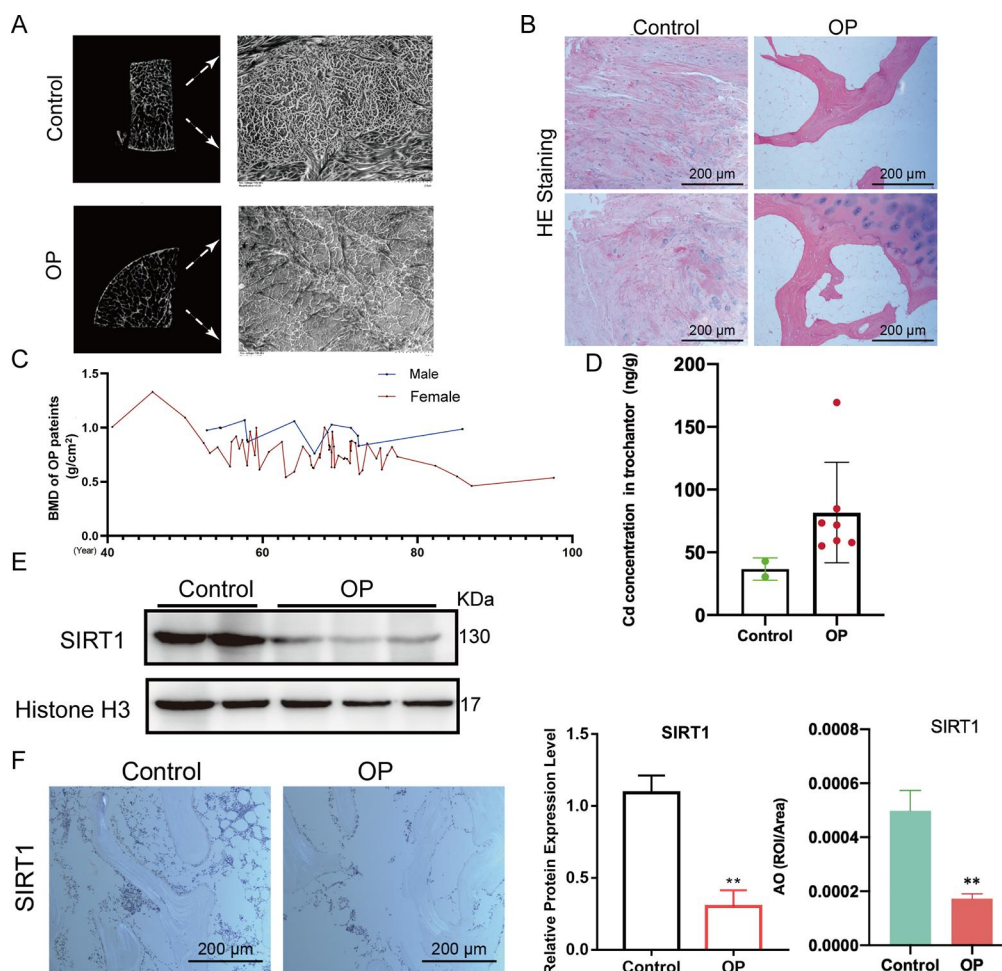


**Figure 1.** Cd accumulation and nuclear SIRT1 inhibition were found in bone tissues of OP patients. (A) Micro-CT of the human femur. Scale bar = 2.0 mm. Trabecular morphology and space were observed by TEM. Scale bar = 2.0  $\mu$ m. (B) H&E staining of the human femur to assess bone tissue damage (20 $\times$ ). (C) BMD values of OP patients. (D) Cd concentrations in human bone tissues were detected by atomic absorption spectroscopy. (E) Nuclear SIRT1 protein expression levels were detected by western blotting and (F) immunohistochemical staining. Multiple comparisons were performed using one-way ANOVA analysis. (\*)  $p < 0.05$  and (\*\*)  $p < 0.01$  compared to the control group.

**Microscopic Computed Tomography (Micro-CT).** The OP patient bone microstructure and the rat bone microstructure were imaged using micro-CT images (SKYSCAN 1174 X-ray Micro-CT, Bruker). Previous described parameters were used for scanning bone tissues,<sup>5</sup> and the region of interest (ROI) was reconstructed using NRecon software.

**Cd Content Detection in Bone Tissues.** Bone tissues were dried at 80  $^{\circ}$ C and dissolved in concentrated nitric acid. After digestion, the samples were diluted in 10 mL of ultrapure water and analyzed with atomic absorption spectroscopy (Optima 7300 DV, PerkinElmer). The quality of the Cd concentration was strictly controlled following the standard reference [SRM1598, National Institute of Standards and Technology (NIST)]. Triplicate readouts were averaged for each group.

**Statistical Analyses.** We use GraphPad Prism 7 (GraphPad Software) to analyze statistics. *In vitro* studies were repeated at least 3 times. For *in vivo* studies, three rats were used to exam relative parameters. All data were analyzed using the one-way analysis of variance (ANOVA) Tukey's *t* test as a post hoc test.  $p < 0.05$  was considered significantly different and presented as the mean  $\pm$  standard deviation (SD).

## RESULTS

**Cd Content Is Increased in the Bone Tissues of OP Patients.** The presence of OP was confirmed by performing micro-CT and TEM (Figure 1A). Spaces of bone trabeculae

were increased histologically by H&E staining (Figure 1B). The prevalence of OP was higher in postmenopausal women than men (Figure 1C), consistent with previous reports. Furthermore, the Cd concentration was significantly increased in the bone of OP patients (Figure 1D). Moreover, the bone tissue of OP patients showed that lower levels of the nuclear SIRT1 protein expression than that of healthy individuals were confirmed by immunohistochemical staining and western blotting (panels E and F of Figure 1). These data indicated that the increase in the Cd concentration was associated with OP development.

**Osteogenesis and Osteoclastogenesis in the Progression of CdCl<sub>2</sub>-Induced OP.** To elucidate Cd-induced OP, first, we established the OP model of rats by bilateral ovariectomy. As shown in Figure 2A, 50 mg/L CdCl<sub>2</sub> exposure for 18 months caused femur plurilocellate, which appears similar to the femur of bilateral ovariectomy rats. Many studies focusing on osteoclasts showed that a high level of osteoclastogenesis is the main reason for OP. However, tartrate-resistant acid phosphatase (TRAP)-positive osteoclasts have no significant changes after CdCl<sub>2</sub> exposure for 18 months in the femur of rats, which is a biomarker of osteoclastogenesis (Figure 2B). Furthermore, to assess osteogenesis and osteoclastogenesis, we measured their related protein ex-

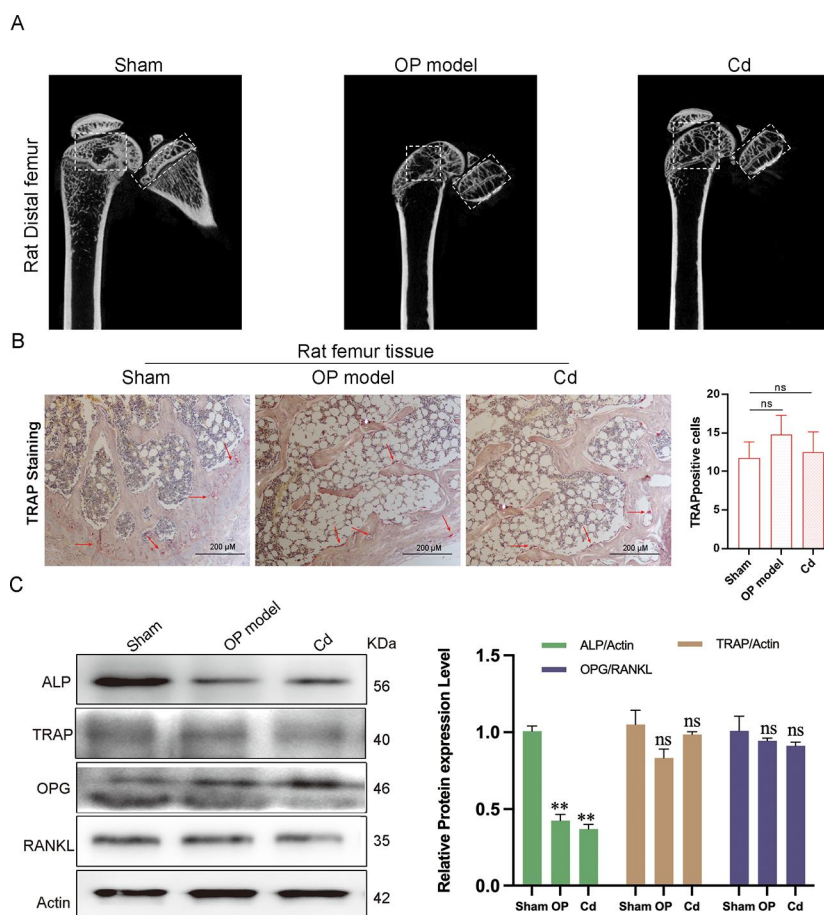


**Figure 2.** Osteogenesis and osteoclastogenesis in OP model rats and CdCl<sub>2</sub>-induced OP rats. (A) Micro-CT of the rat distal femur. (B) TRAP staining of rat femur tissues. (C) Protein expression of ALP and TRAP and OPG/RANKL ratio in the femur of rats ( $n = 10/\text{group}$ ). Multiple comparisons were performed using one-way ANOVA analysis. (\*)  $p < 0.05$  and (\*\*)  $p < 0.01$  compared to the sham group.

pression levels by western blotting. Interestingly, the alkaline phosphatase (ALP) protein expression level, a vital osteogenesis biomarker, was significantly decreased after CdCl<sub>2</sub> exposure (Figure 2C). Meanwhile, the TRAP expression level and ratio of osteoprotegerin (OPG) and receptor activator of NF- $\kappa$ B ligand (RANKL) expression showed no significant changes in the CdCl<sub>2</sub> exposure group. When taken together, these data convincingly indicated that 50 mg/L CdCl<sub>2</sub> exposure for 18 months caused rat OP through inhibition of osteogenesis rather than active osteoclastogenesis.

**Nuclear SIRT1-Acetylated P53 Was Involved in CdCl<sub>2</sub> Exposure-Induced Osteoblast Apoptosis.** To reveal underlying mechanisms involved in Cd-induced OP in osteoblasts, we used a candidate-based strategy to test whether some gene regulation pathways mediate this process. As shown in Figure 3A, nuclear SIRT1 gradually decreased as the concentration of CdCl<sub>2</sub> increased. In contrast, its substrate PGC-1 $\alpha$  and the acetylation of P53 at lysine 382 gradually increased. For further validation of SIRT1-overexpressed osteoblasts, PGC-1 $\alpha$  and P53<sup>Lys382</sup> protein levels of treated cells were tested using western blotting. Indeed, the levels of PGC-1 $\alpha$  and P53<sup>Lys382</sup> in the group of SIRT1 overexpression + CdCl<sub>2</sub> treatment were lower when compared to the Cd group (Figure 3B).

Additionally, the apoptosis of osteoblasts with CdCl<sub>2</sub> treatment was significantly higher than that of the control group using flow cytometry (Figure 3C), and the western blot

(Figure 3D) illustrated that cleaved caspase 9, cleaved caspase 3, and the Bax/Bcl-2 ratio were upregulated in the CdCl<sub>2</sub>-treated groups than in the SIRT1 overexpression + Cd-treated group (panels E and F of Figure 3). The data of this study reveal that SIRT1 overexpression protects CdCl<sub>2</sub>-treated osteoblasts by deacetylating P53 at lysine 382 to slow apoptosis.

#### ROS–SIRT1 Cyclic Signaling Pathway Regulates Caspase-Dependent Apoptosis after CdCl<sub>2</sub> Exposure.

Excessive osteoblast apoptosis correlates with oxidative stress, causing decreased osteogenesis.<sup>23</sup> The production of ROS was detected by DCFH-DA staining after the treatment of different concentrations of CdCl<sub>2</sub> by flow cytometry. The results showed that osteoblasts treated with higher concentrations of CdCl<sub>2</sub> groups generated more ROS (Figure 4A). To investigate the antioxidant capacity of the osteoblasts, we measured the content of MDA and SOD activity. Panels B and C of Figure 4 showed that the MDA content of osteoblasts in a higher concentration of CdCl<sub>2</sub> groups was significantly increased. In contrast, the activity of SOD was significantly decreased. Furthermore, as presented in panels D–F of Figure 4, NAC obviously alleviated CdCl<sub>2</sub>-elevated ROS and MDA content levels and increased SOD activity in osteoblasts. According to these experiments, CdCl<sub>2</sub> exposure can cause oxidative stress in osteoblasts. Here, we proposed a hypothesis that Cd exposure caused osteoblast apoptosis through ROS-mediated nuclear SIRT1 inhibition.

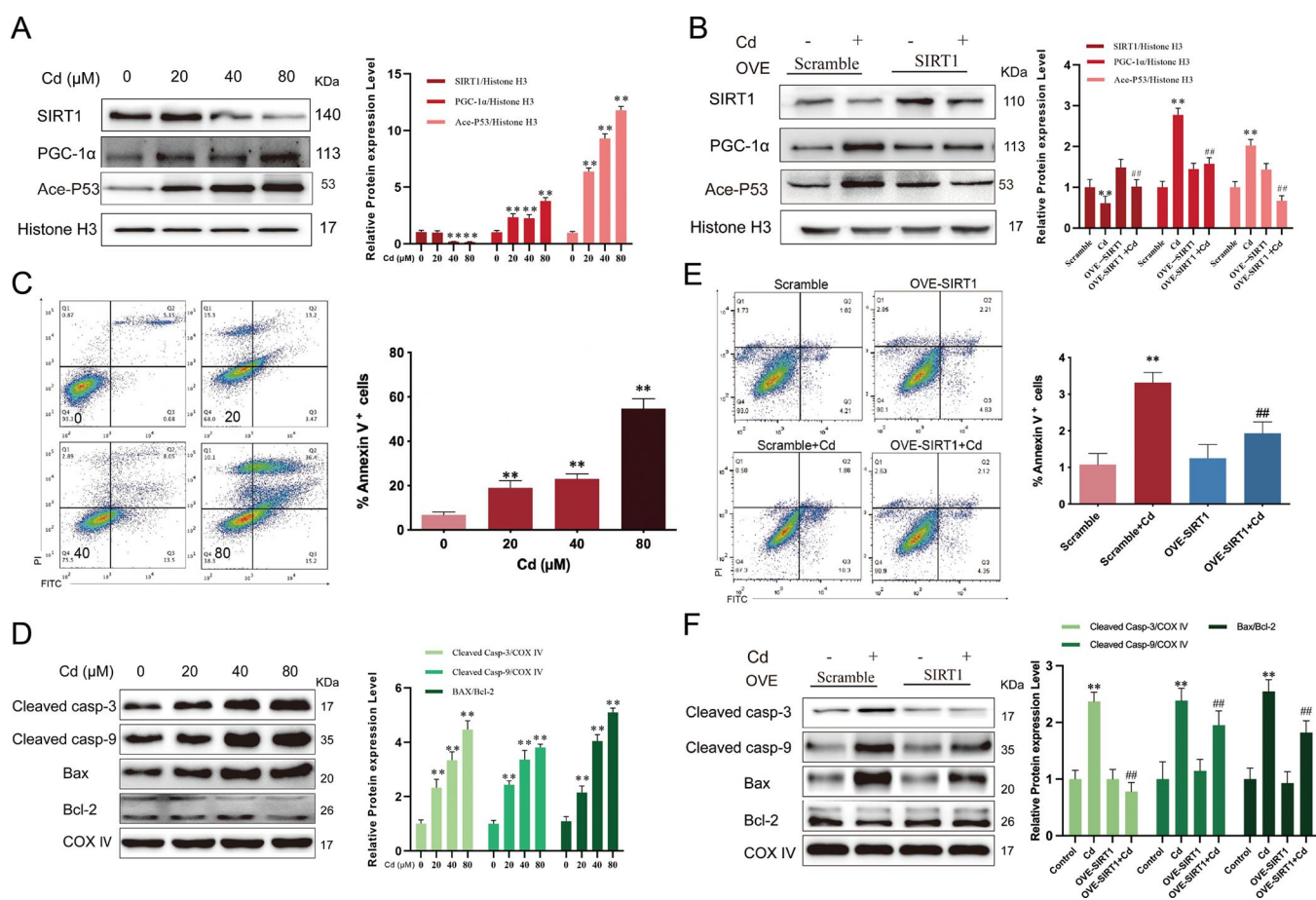


**Figure 3.** Effects of nuclear SIRT1 overexpression in CdCl<sub>2</sub>-induced apoptosis of osteoblast. (A and B) ROS1728 cells were treated with CdCl<sub>2</sub> (0, 20, 40, and 80 μM) for 6 h. SIRT1-overexpressed ROS1728 cells were established and exposed to 40 μM CdCl<sub>2</sub> for 6 h. Nuclear protein expression of SIRT1, PGC-1α, and Ace-P53 were detected by western blotting. (C and E) Annexin V<sup>+</sup> cells were detected by flow cytometry. (D and F) Mitochondrial proteins of cleaved caspase 9 and cleaved caspase 3 and Bax/Bcl-2 ratio was detected by western blotting. Multiple comparisons were performed using one-way ANOVA analysis. (\*)  $p < 0.05$  and (\*\*)  $p < 0.01$  compared to the control group, and (#)  $p < 0.05$  and (##)  $p < 0.01$  compared to the CdCl<sub>2</sub> group.

Interestingly, SIRT1 overexpression reduced Cd-induced ROS release (Figure 4H). Meanwhile, the MDA content decreased and SOD activity increased in the OVE-SIRT1 + Cd group compared to the Cd group (panels I and J of Figure 4). Furthermore, the result of western blotting revealed that the expression levels of cleaved caspase 9 and cleaved caspase 3 and the ratio of Bax/Bcl-2 proteins were significantly reduced in the rat femur from the NAC + Cd and OVE-SIRT1 + Cd groups when compared to the Cd group (Figure 4K). When taken together, these data showed that the ROS–SIRT1 cyclic signaling pathway regulates caspase-dependent apoptosis in response to Cd-induced OP.

**SIRT1 Overexpression Attenuated CdCl<sub>2</sub>-Induced OP in Rats.** Micro-CT three-dimensional (3D) images of the distal femur and trabecular bone assessed the effects of SIRT1 overexpression on Cd-induced OP. Notably, SIRT1 overexpression reversed the Cd-exposure-lowered BMD, trabecular bone parameters (Tb.Sp and Tb.Th), and bone mass parameter (BV/TV) in rats (panels A and B of Figure 5). We further confirmed that Cd exposure caused OP, with the ultrastructural and pathological changes in the trabecular bone by TEM and H&E staining (panels A and B of Figure 6). As expected, SIRT1 overexpression attenuated Cd exposure, causing disordered bone trabeculae, decreased spaces of bone trabeculae, and numerous broken trabecular bones. Mean-

while, results by immunohistochemistry (IHC) showed that the ALP protein expression level was significantly reduced in the rat femur from the OVE-SIRT1 + Cd group when compared to the Cd group (panels C and D of Figure 6). Correspondingly, the use of antioxidant NAC effectively reversed Cd-induced OP, indicating that oxidative stress plays a vital role in this progression.

In addition, Cd induced apoptosis via ROS release and SIRT1–P53<sup>Lys382</sup> signaling pathway activation. The nuclear SIRT1, PGC-1α, and P53<sup>Lys382</sup> protein expression levels and caspase-dependent apoptosis-related protein expression levels were observed in the rat femur. As shown in Figure 7A, in comparison to the Cd group, the SIRT1 protein expression level in rat femur tissues increased, observed in NAC + Cd and OVE-SIRT1 + Cd groups, and PGC-1α and P53<sup>Lys382</sup> protein expression levels were suppressed. Mechanistically, the above data indicated that ROS–SIRT1 signaling regulated caspase-dependent apoptosis in response to Cd-induced OP (Figure 7B).

## DISCUSSION

OP is a systemic disease characterized by low BMD and microarchitectural deterioration of bone tissue, leaving affected bones vulnerable to fracture.<sup>24</sup> Osteoblast lineage derives from

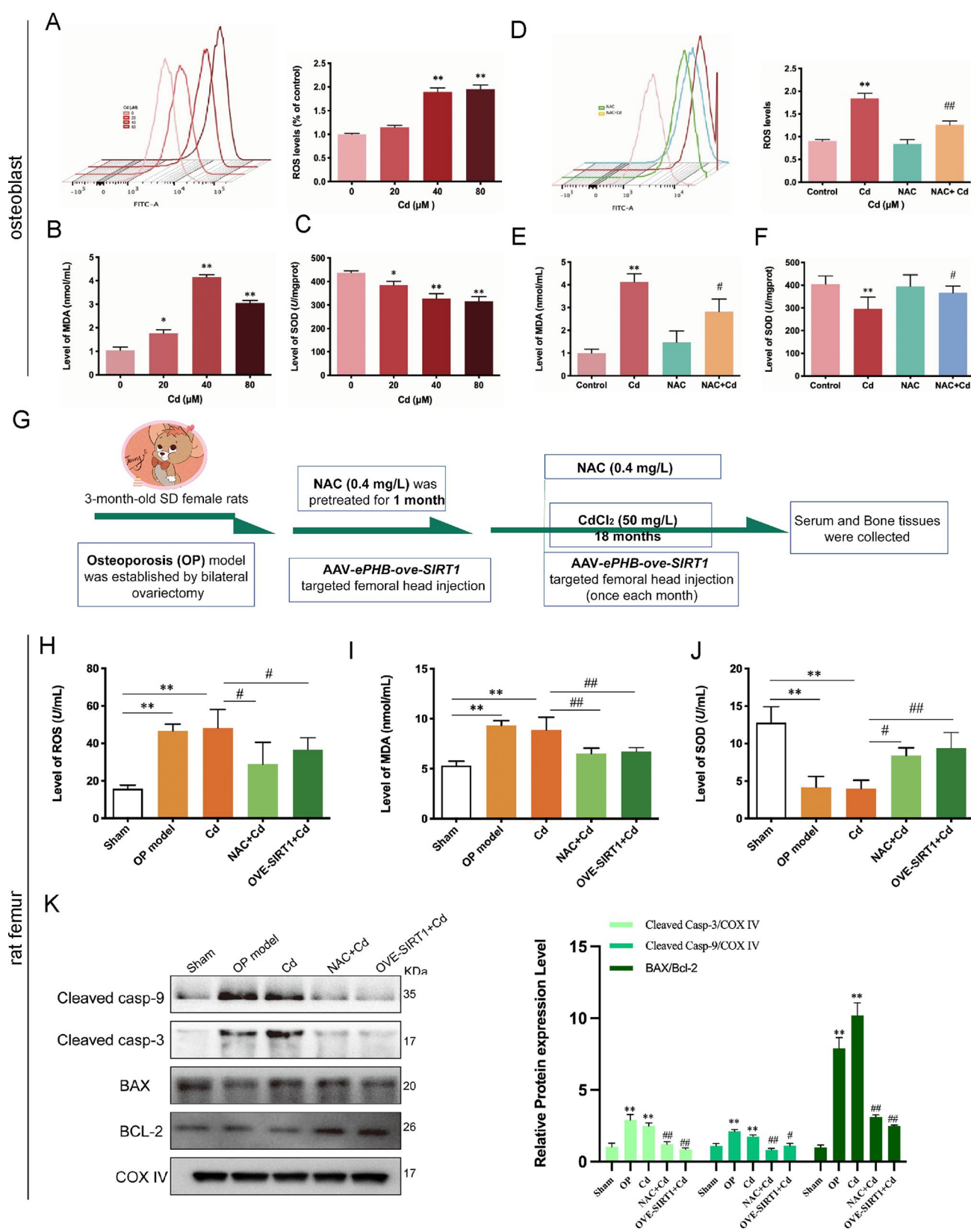


**Figure 4.** Effects of NAC in Cd-induced SIRT1 inhibition and apoptosis both *in vivo* and *in vitro*. ROS1728 cells were exposed to CdCl<sub>2</sub> (20, 40, and 80  $\mu$ M), or SIRT1-overexpressed ROS1728 cells were exposed to 40  $\mu$ M for 6 h. (A and D) Intracellular ROS were detected by flow cytometry. (B and E) MDA content and (C and F) SOD activity was detected by the ELISA kit. (G) Experimental flow chart. (H–J) Rat serum ROS generation, MDA content, and SOD activity were detected by ELISA kits. (K) Mitochondrial proteins of cleaved caspase 9 and cleaved caspase 3 and Bax/Bcl-2 ratio was detected by western blotting. Multiple comparisons were performed using one-way ANOVA analysis. (\*)  $p < 0.05$  and (\*\*)  $p < 0.01$  compared to the sham group, and (#)  $p < 0.05$  and (##)  $p < 0.01$  compared to the Cd group.

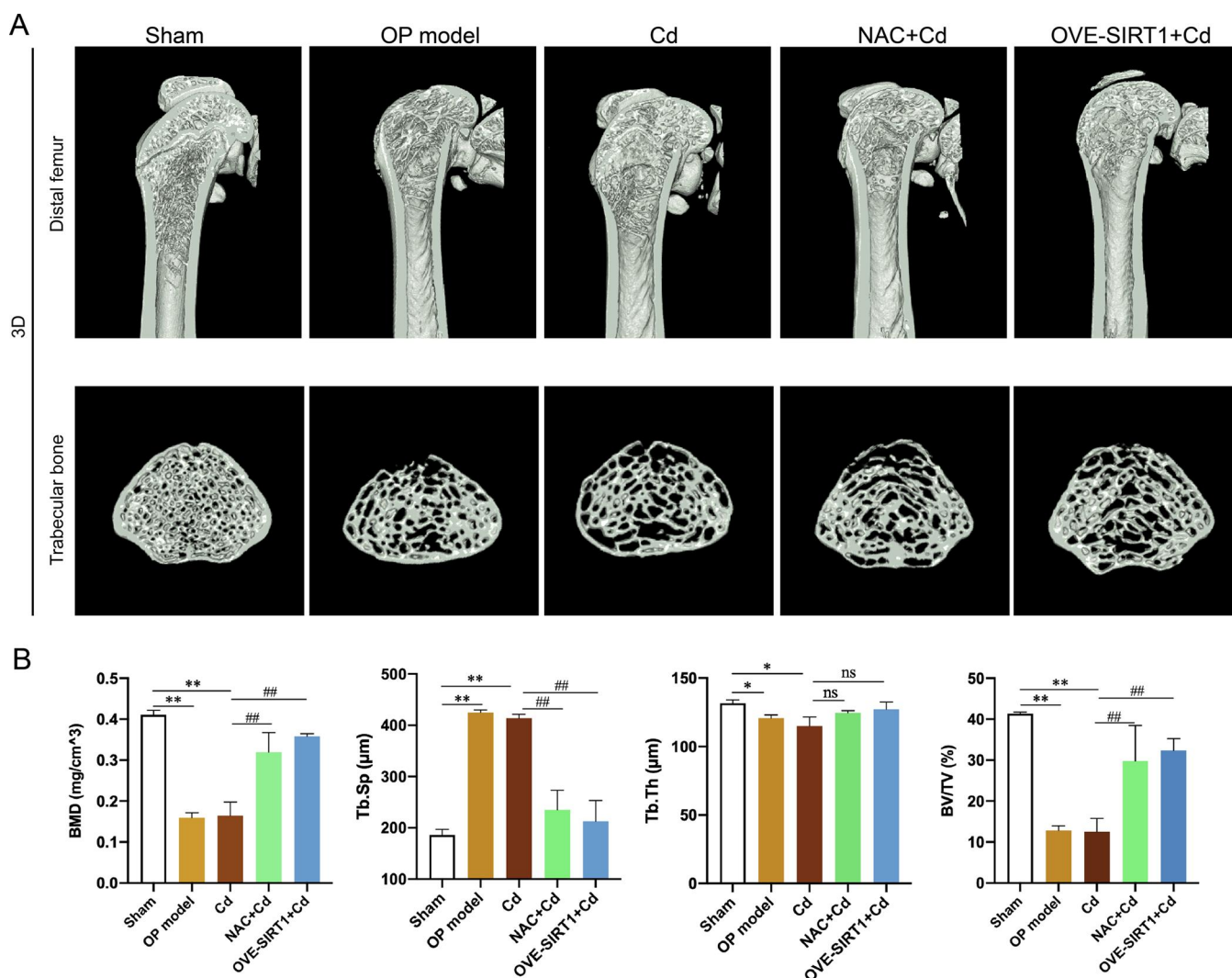


**Figure 5.** SIRT1 overexpression attenuated Cd-induced bone loss in rats. (A) 3D reconstruction micro-CT results showed the amount of trabecular bone and spine. (B) Some parameters including BMD, Tb.Sp, Tb.Th, and BV/TV for OP. Multiple comparisons were performed using one-way ANOVA analysis. (\*)  $p < 0.05$  and (\*\*)  $p < 0.01$  compared to the sham group, and (#)  $p < 0.05$  and (##)  $p < 0.01$  compared to the Cd group.

the differentiation of mesenchymal cells in the stromal compartment of bone marrow (BM). The BM stroma contains self-renewing, multipotent progenitors that can give rise to osteoblasts, thus ensuring a reservoir of bone-forming cells for bone growth, modeling, and remodeling.<sup>25</sup> Bone homeostasis depends upon the precise balance between bone resorption by osteoclasts and bone formation by osteoblasts, which include a series of complex and highly regulated steps. The disruption of bone homeostasis is an essential aspect of the pathogenesis of OP.<sup>26</sup> It has been well-established that Cd exposure can cause itai-itai disease and lead to bone fracture and OP.<sup>27</sup> In the study by Alfvén et al., decreased bone mineral density with increasing blood Cd has been described in a few studies, and they also found a high level of Cd accumulation in bone tissues of OP patients, even reaching about 170 ng/g (Figure 1B). Cd-contaminated food in many areas is a high risk to human health.<sup>28</sup> Environmental Cd is easily taken up in animal and human bodies through the food chain, and tobacco smoking further increases Cd exposure. The survey found that the risk was increased in a geographical area with high Cd pollution compared to an area with low Cd pollution and in relation to

the Cd concentrations in soil.<sup>28</sup> Many of the *in vivo* models indicated different levels of bone loss depending upon Cd dose and exposure periods as well as differences between rats, mice, and humans.<sup>5,29</sup> We carried out 18 months of CdCl<sub>2</sub> exposure in rats and found that CdCl<sub>2</sub> induction can lead to changes in trabecular morphology and microstructure, decreased bone density, and expression of ALP. Additionally, TRAP staining showed CdCl<sub>2</sub> exposure has no significant effect on the number of osteoclasts in the femur of rats.

ALP is highly expressed in osteoblasts and plays a critical function in the formation of bone tissue.<sup>30</sup> In CdCl<sub>2</sub>-induced OP model rats, NAC and SIRT1 overexpression increased ALP expression levels in bone tissues, confirming the effect in promoting osteogenesis (Figure 4H). TRAP is considered just a histochemical marker of osteoclasts. However, TRAP staining showed no significant change in the number of osteoclasts in OP rats (Figure 4F). This appears to be a contradiction, because increased osteoclast activity is considered the culprit in OP.<sup>31</sup> A CdCl<sub>2</sub>-induced increase in the activity of caspase-3 may cause osteoblast death, and the indirect mechanism is interfering with calcium (Ca), phosphorus (P), vitamin D, and

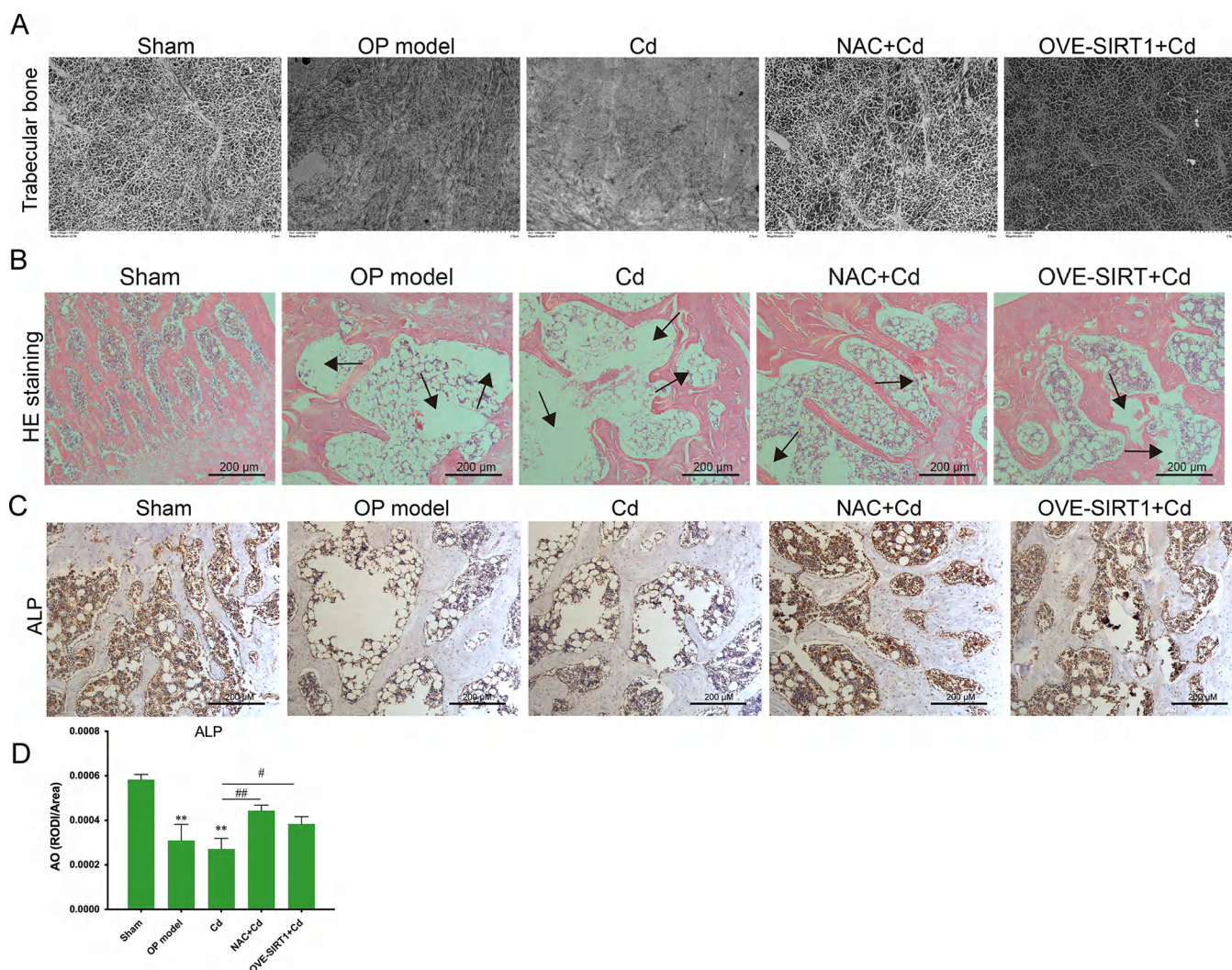


**Figure 6.** SIRT1 overexpression attenuated Cd-induced breaking of the microstructure of the trabecular bone and reduction of ALP in the rat femur. (A) Microstructures of the trabecular bone were observed by TEM. (B) H&E staining of the human femur to assess bone tissue damage (20 $\times$ ). (C and D) ALP protein expression level was detected by immunohistochemical staining. Multiple comparisons were performed using one-way ANOVA analysis. (\*)  $p < 0.05$  and (\*\*)  $p < 0.01$  compared to the sham group, and (#)  $p < 0.05$  and (##)  $p < 0.01$  compared to the Cd group.

renal dysfunction.<sup>32</sup> Our previous study found that a low dose of CdCl<sub>2</sub> decreased the osteoclast apoptosis rate *in vitro*.<sup>5</sup> However, the present study is the first report that long-term CdCl<sub>2</sub> exposure failed to increase the osteoclast number and bone resorption *in vivo*. It is well-known that osteoclasts and osteoblasts are involved in the bone homeostasis and remodeling process. There are complex mutual signaling regulations between osteoclasts and osteoblasts; for instance, osteoblast-secreted RANKL and its decoy receptor, OPG, are essential for promoting osteoclast differentiation and inhibiting bone formation.<sup>33</sup> Bone resorption conducted by osteoclasts is accomplished in a reasonably short time relative to that required for bone formation by osteoblasts.<sup>34</sup> Therefore, long-term CdCl<sub>2</sub>-exposure-induced osteoblast damage is a key cause of the progression of OP.

*In vivo* stimulation of SIRT1 can extend the lifespan of mice and protect against a number of aging-related diseases, including OP.<sup>35,36</sup> Many mouse models also indicate that SIRT1 regulates bone modeling and remodeling, and its agonists can protect against age-related, postmenopausal, and disuse models of OP, and SIRT1 knockout models display low bone mass phenotypes associated with increased bone

resorption and decreased bone formation.<sup>37–39</sup> In recent years, serious SIRT1 drugs are in clinical trials and are shown to be safe and have salutary effects on bone mass in humans.<sup>39</sup> However, how SIRT1 exerts its function via hormone signaling or direct action in osteoblasts is not fully understood. Interestingly, the effects of deleting SIRT1 in different cell types, including in osteoclasts and osteoblasts, may not be simply additive.<sup>40</sup> Resveratrol was the first-generation SIRT1 agonist, and mice treated with resveratrol for more than 18 months showed modest improvements in bone mass, indicating partial protection against aging-related OP.<sup>35</sup> The mechanism of the regulation of the SIRT1–P53 axis and pertinent pathways are pivotal. As a NAD-dependent deacetylase, we indicated that Cd exposure downregulated the expression level of SIRT1 through deacetylating P53. There were many reports that heavy metals, including cadmium, lead, and arsenic, as environmental pollutants induce oxidative stress and produce ROS, leading to harmful effects on different tissues, including liver, brain, and bone tissues.<sup>41</sup> Although there is evidence that oxidative stress is an essential driver of OP, the multilevel interacting factors and pathways are incompletely understood. The present study

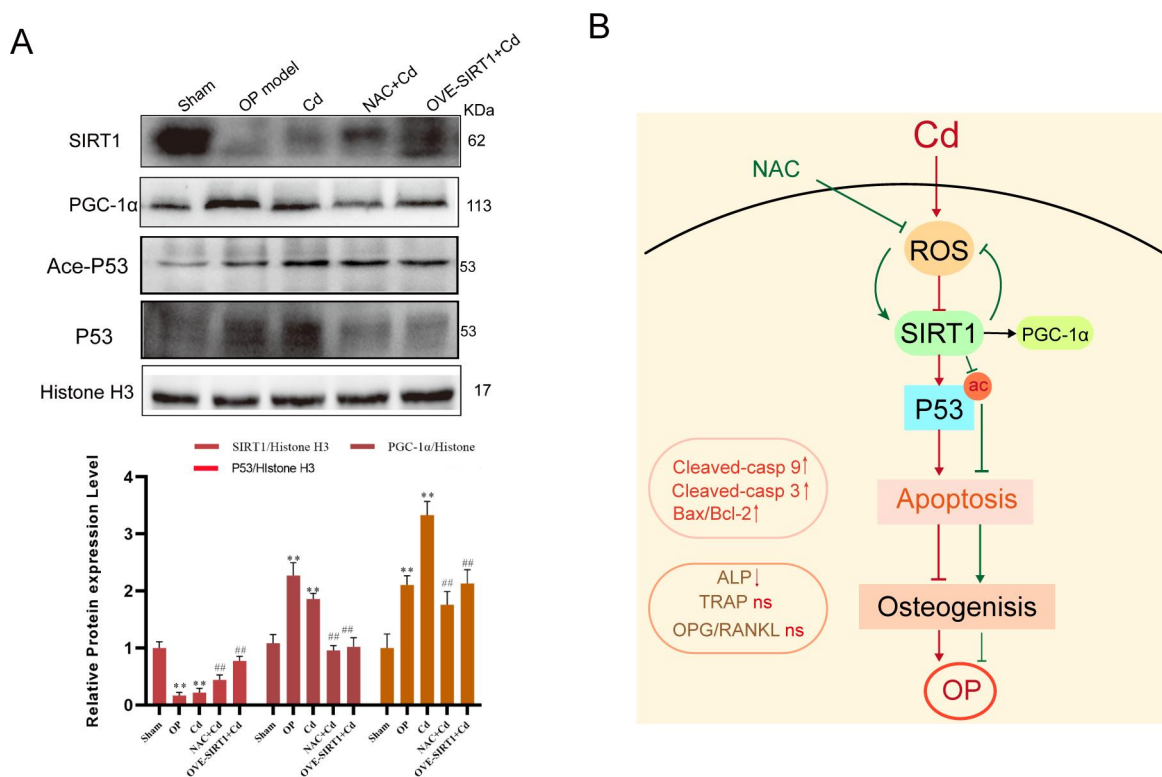


**Figure 7.** SIRT1 overexpression reversed Cd exposure that caused SIRT1 inhibition and apoptosis of rat femur. (A) Nuclear SIRT1, PGC-1 $\alpha$ , and Ace-P53 protein expression levels in rat femur tissues were detected by western blotting. (B) Signaling cascade involved in CdCl<sub>2</sub>-induced OP. Multiple comparisons were performed using one-way ANOVA analysis. (\*)  $p < 0.05$  and (\*\*)  $p < 0.01$  compared to the sham group, and (#)  $p < 0.05$  and (##)  $p < 0.01$  compared to the Cd group.

justified the oxidative stress, and caspase-dependent apoptosis that subsequently occurs has been linked to SIRT1 inhibition in the progression of CdCl<sub>2</sub>-induced OP. The crosstalk between ROS and endogenous mitochondrial apoptosis is connected with the acetylation of P53 by nuclear SIRT1 (Figures 3B and 7A).

SIRT1 deacetylates the P53 tumor suppressor protein to dampen apoptotic and cellular senescence pathways.<sup>38</sup> SIRT1 overexpression inhibited P53 transcriptional activity and P53-dependent apoptosis in response to DNA damage and oxidative stresses.<sup>42</sup> Furthermore, in response to DNA damage and other cellular stresses, P53 is stabilized and activated to trigger apoptosis and cell-cycle arrest.<sup>43</sup> Consistently, our observations provide direct evidence that nuclear SIRT1 protein regulates P53 acetylation, and caspase-dependent apoptosis shows that the function of nuclear SIRT1 is required for antioxidation in CdCl<sub>2</sub>-induced OP processes. Alternatively, in addition to deacetylating P53, SIRT1 could regulate other signaling pathways, including PGC-1 $\alpha$ , FOXO1, FOXO3, Ku70, NF- $\kappa$ B, and AceCS1, to regulate physiological processes, such as stress resistance and energy metabolism, that are known to be affected during aging and OP.<sup>44</sup> Anderson et al. verified that PGC-1 $\alpha$  is found in both the nucleus and cytoplasm and translocated to the nucleus during stress.<sup>45</sup> PGC-1 $\alpha$  is a master transcriptional regulator of mitochondrial function, which is located and perpetually active in the nucleus, and Cd exposure increased its expression level in osteoblast and rat bone tissues as well as in bone tissues of OP patients (Figure 7A). PGC-1 $\alpha$  is capable of improving or rescuing mitochondrial dysfunction, and it is also involved in regulating genes related with ROS scavenging.<sup>46</sup> This study demonstrated

that the ROS and MDA levels were increased while the activities of SOD were decreased in the Cd group, which are common indicators of oxidative stress.<sup>47</sup> In the current study, NAC and SIRT1 overexpression could inhibit P53 acetylation at lysine 382 and nuclear PGC-1 $\alpha$  in bone tissues of OP patients (panels E and F of Figure 1). It is well-known that PGC-1 $\alpha$  is sufficient to handle an effect on mitochondrial function through an increase, and mitochondria regulation is a stress response component. These findings indicate that PGC-1 $\alpha$  regulated by SIRT1 inhibition plays a role in the regulation of mitochondria, which is a component of the oxidative stress response. However, our results cannot illustrate the mechanism of the regulation of mitochondrial function mediated by PGC-1 $\alpha$ . It was reported that the SIRT1 non-specific inhibitors, nicotinamide and sirtinol, have increased PGC-1 $\alpha$  acetylation by inhibition of SIRT1 in response to oxidative stress.<sup>48</sup>

Meanwhile, we cannot rule out the possibility that other sirtuins function in oxidative stress and contribute to the effect of mitochondria function. Mitochondria play a crucial role in apoptosis by activating mitochondrial outer membrane permeabilization, which leads to the release of caspase-activating molecules, caspase-independent death effectors, and disruption of ATP production.<sup>49</sup> Despite the central role for mitochondria in the control of apoptosis, surprisingly little is known about how nuclear SIRT1 participates in apoptotic programs. It was observed that the SIRT1/PGC-1 $\alpha$ /P53<sup>Lys382</sup> signaling pathway was involved in the activation of oxidative mitochondrial apoptosis signaling. However, PGC-1 $\alpha$  as a master regulator of mitochondrial biogenesis and function is responsive to a variety of metabolic stresses.<sup>50</sup> Furthermore, the phenomena were observed that SIRT1 overexpression

treatment attenuated CdCl<sub>2</sub>-induced mitochondrial apoptosis in osteoblast and bone tissues, implying this inference, as shown in panels C, E, and F of Figure 3. Thus, this study verified a signaling cascade in apoptosis caused by CdCl<sub>2</sub> exposure, as described in Figure 7B. In conclusion, nuclear SIRT1 regulates P53 acetylation at lysine 382, participating in oxidative damage; meanwhile, the SIRT1/PGC-1 $\alpha$  pathway plays a role in the regulation of mitochondria apoptosis. Thus, it is clear that the ROS–SIRT1 cyclic signaling pathway regulated apoptosis and plays a curial role in the maintenance of normal bone homeostasis and the onset of OP caused by CdCl<sub>2</sub>.

## AUTHOR INFORMATION

### Corresponding Authors

**Hui Zou** – College of Veterinary Medicine, Yangzhou University, Yangzhou, Jiangsu 225009, People's Republic of China; Jiangsu Co-Innovation Center for Prevention and Control of Important Animal Infectious Diseases and Zoonoses, Yangzhou, Jiangsu 225009, People's Republic of China; Email: [zouhui@yzu.edu.cn](mailto:zouhui@yzu.edu.cn)

**Zongping Liu** – College of Veterinary Medicine, Yangzhou University, Yangzhou, Jiangsu 225009, People's Republic of China; Jiangsu Co-Innovation Center for Prevention and Control of Important Animal Infectious Diseases and Zoonoses, Yangzhou, Jiangsu 225009, People's Republic of China; [orcid.org/0000-0001-9071-8363](https://orcid.org/0000-0001-9071-8363); Email: [liuzongping@yzu.edu.cn](mailto:liuzongping@yzu.edu.cn)

### Authors

**Di Ran** – College of Veterinary Medicine, Southwest University, Chongqing 400715, People's Republic of China; College of Veterinary Medicine, Yangzhou University, Yangzhou, Jiangsu 225009, People's Republic of China; Jiangsu Co-Innovation Center for Prevention and Control of Important Animal Infectious Diseases and Zoonoses, Yangzhou, Jiangsu 225009, People's Republic of China

**Dehui Zhou** – College of Veterinary Medicine, Yangzhou University, Yangzhou, Jiangsu 225009, People's Republic of China; Jiangsu Co-Innovation Center for Prevention and Control of Important Animal Infectious Diseases and Zoonoses, Yangzhou, Jiangsu 225009, People's Republic of China

**Gang Liu** – Department of Pathology & Laboratory Medicine, Tulane University School of Medicine, New Orleans, Louisiana 70112, United States

**Yonggang Ma** – College of Veterinary Medicine, Yangzhou University, Yangzhou, Jiangsu 225009, People's Republic of China; Jiangsu Co-Innovation Center for Prevention and Control of Important Animal Infectious Diseases and Zoonoses, Yangzhou, Jiangsu 225009, People's Republic of China

**Waseem Ali** – College of Veterinary Medicine, Yangzhou University, Yangzhou, Jiangsu 225009, People's Republic of China; Jiangsu Co-Innovation Center for Prevention and Control of Important Animal Infectious Diseases and Zoonoses, Yangzhou, Jiangsu 225009, People's Republic of China

**Rui Yu** – College of Veterinary Medicine, Yangzhou University, Yangzhou, Jiangsu 225009, People's Republic of China; Jiangsu Co-Innovation Center for Prevention and Control of Important Animal Infectious Diseases and Zoonoses, Yangzhou, Jiangsu 225009, People's Republic of China

**Qinghua Wang** – College of Veterinary Medicine, Southwest University, Chongqing 400715, People's Republic of China; [orcid.org/0000-0003-4669-3458](https://orcid.org/0000-0003-4669-3458)

**Hongyan Zhao** – College of Veterinary Medicine, Yangzhou University, Yangzhou, Jiangsu 225009, People's Republic of China; Jiangsu Co-Innovation Center for Prevention and Control of Important Animal Infectious Diseases and Zoonoses, Yangzhou, Jiangsu 225009, People's Republic of China

**Jiaqiao Zhu** – College of Veterinary Medicine, Yangzhou University, Yangzhou, Jiangsu 225009, People's Republic of China; Jiangsu Co-Innovation Center for Prevention and Control of Important Animal Infectious Diseases and Zoonoses, Yangzhou, Jiangsu 225009, People's Republic of China

Complete contact information is available at:

<https://pubs.acs.org/10.1021/acs.jafc.2c08505>

### Author Contributions

<sup>†</sup>Hui Zou and Zongping Liu contributed equally to this work.

### Funding

This work was supported by the Fundamental Research Funds for the Central Universities (SWU-KQ22056), the National Natural Science Foundation of China (31872533, 31902329, 32072933, 31702304, and 32172923), the National Key Research and Development Program of China (2016YFD0501208), and the Project of the Priority Academic Program Development of Jiangsu Higher Education Institution (PADD).

### Notes

The authors declare no competing financial interest.

## REFERENCES

- (1) Nishijo, M.; Nakagawa, H.; Suwazono, Y.; Nogawa, K.; Kido, T. Causes of death in patients with Itai-itai disease suffering from severe chronic cadmium poisoning: A nested case-control analysis of a follow-up study in Japan. *BMJ Open* **2017**, *7*, e015694.
- (2) Satarug, S.; Baker, J. R.; Urbenjapol, S.; Haswell-Elkins, M.; Reilly, P. E. B.; Williams, D. J.; Moore, M. R. A global perspective on cadmium pollution and toxicity in non-occupationally exposed population. *Toxicol. Lett.* **2003**, *137* (1), 65–83.
- (3) Zamoiski, R. D.; Guallar, E.; Garcia-Vargas, G. G.; Rothenberg, S. J.; Resnick, C.; Andrade, M. R.; Steuerwald, A. J.; Parsons, P. J.; Weaver, V. M.; Navas-Acien, A.; Silbergeld, E. K. Association of arsenic and metals with concentrations of 25-hydroxyvitamin D and 1,25-dihydroxyvitamin D among adolescents in Torreón, Mexico. *Environ. Health Perspect.* **2014**, *122*, 1233–1238.
- (4) Galvez-Fernandez, M.; Grau-Perez, M.; Garcia-Barrera, T.; Ramirez-Acosta, S.; Gomez-Ariza, J. L.; Perez-Gomez, B.; Galan-Labaca, I.; Navas-Acien, A.; Redon, J.; Briongos-Figuero, L. S.; Dueñas-Laita, A.; Perez-Castrillon, J. L.; Tellez-Plaza, M.; Martin-Escudero, J. C. Arsenic, cadmium, and selenium exposures and bone mineral density-related endpoints: The HORTEGA study. *Free Radical Biol. Med.* **2021**, *162*, 392–400.
- (5) Ma, Y.; Ran, D.; Shi, X.; Zhao, H.; Liu, Z. Cadmium toxicity: A role in bone cell function and teeth development. *Sci. Total Environ.* **2021**, *769*, 144646.
- (6) Buha, A.; Jugdaohsingh, R.; Matovic, V.; Bulat, Z.; Antonijevic, B.; Kerns, J. G.; Goodship, A.; Hart, A.; Powell, J. J. Bone mineral health is sensitively related to environmental cadmium exposure—Experimental and human data. *Environ. Res.* **2019**, *176*, 108539.

- (5) Ma, Y.; Ran, D.; Cao, Y.; Zhao, H.; Song, R.; Zou, H.; Gu, J.; Yuan, Y.; Bian, J.; Zhu, J.; Liu, Z. The effect of P2X7 on cadmium-induced osteoporosis in mice. *J. Hazard. Mater.* **2021**, *405*, 124251.
- (6) Yang, Y.; Cheng, R.; Liu, J.; Fang, J.; Wang, X.; Cui, Y.; Zhang, P.; Du, B. Lincrin Protects against Cadmium-Induced Osteoporosis Via Reducing Oxidative Stress and Inflammation and Altering RANK/RANKL/OPG Pathway. *Biol. Trace Elem. Res.* **2022**, *200*, 3688.
- (7) Ma, Y.; Ran, D.; Zhao, H.; Song, R.; Zou, H.; Gu, J.; Yuan, Y.; Bian, J.; Zhu, J.; Liu, Z. Cadmium exposure triggers osteoporosis in duck via P2X7/PI3K/AKT-mediated osteoblast and osteoclast differentiation. *Sci. Total Environ.* **2021**, *750*, 141638. Kaji, T.; Takata, M.; Miyahara, T.; Kozuka, H.; Koizumi, F. Interaction of zinc with cadmium and copper on ossification of embryonic chick bone in tissue culture. *Arch. Environ. Contam. Toxicol.* **1990**, *19* (5), 653–656.
- (8) Ezaki, T.; Tsukahara, T.; Moriguchi, J.; Furuki, K.; Fukui, Y.; Ukai, H.; Okamoto, S.; Sakurai, H.; Honda, S.; Ikeda, M. No clear-cut evidence for cadmium-induced renal tubular dysfunction among over 10,000 women in the Japanese general population: A nationwide large-scale survey. *Int. Arch. Occup. Environ. Health* **2003**, *76* (3), 186–196.
- (9) Zeng, Q.; Li, N.; Wang, Q.; Feng, J.; Sun, D.; Zhang, Q.; Huang, J.; Wen, Q.; Hu, R.; Wang, L.; Ma, Y.; Fu, X.; Dong, S.; Cheng, X. The Prevalence of Osteoporosis in China, a Nationwide, Multicenter DXA Survey. *J. Bone Miner. Res.* **2019**, *34*, 1789–1797. Li, Q.; Cheng, J. C.-Y.; Jiang, Q.; Lee, W. Y.-W. Role of sirtuins in bone biology: Potential implications for novel therapeutic strategies for osteoporosis. *Aging Cell* **2021**, *20*, e13301. Gullberg, B.; Johnell, O.; Kanis, J. A. World-wide projections for hip fracture. *Osteoporosis Int.* **1997**, *7*, 407–413. Patel, J. Economic implications of osteoporotic fractures in postmenopausal women. *Am. J. Manage. Care* **2020**, *26*, S311–S318.
- (10) Wan, M.; Gray-Gaillard, E. F.; Elisseeff, J. H. Cellular senescence in musculoskeletal homeostasis, diseases, and regeneration. *Bone Res.* **2021**, *9*, 41.
- (11) Cheng, H.-L.; Mostoslavsky, R.; Saito, S.; Manis, J. P.; Gu, Y.; Patel, P.; Bronson, R.; Appella, E.; Alt, F. W.; Chua, K. F. Developmental defects and p53 hyperacetylation in Sir2 homolog (SIRT1)-deficient mice. *Proc. Natl. Acad. Sci. U. S. A.* **2003**, *100*, 10794–10799.
- (12) McBurney, M. W.; Yang, X.; Jardine, K.; Hixon, M.; Boekelheide, K.; Webb, J. R.; Lansdorp, P. M.; Lemieux, M. The mammalian SIR2 $\alpha$  protein has a role in embryogenesis and gametogenesis. *Mol. Cell. Biol.* **2003**, *23*, 38–54.
- (13) Cohen, D. E.; Supinski, A. M.; Bonkowski, M. S.; Donmez, G.; Guarente, L. P. Neuronal SIRT1 regulates endocrine and behavioral responses to calorie restriction. *Genes Dev.* **2009**, *23*, 2812–2817.
- (14) Artsi, H.; Cohen-Kfir, E.; Gurt, I.; Shahar, R.; Bajayo, A.; Kalish, N.; Bellido, T. M.; Gabet, Y.; Dresner-Pollak, R. The Sirtuin1 activator SRT3025 down-regulates sclerostin and rescues ovariectomy-induced bone loss and biomechanical deterioration in female mice. *Endocrinology* **2014**, *155*, 3508–3515. Feng, J.; Liu, S.; Ma, S.; Zhao, J.; Zhang, W.; Qi, W.; Cao, P.; Wang, Z.; Lei, W. Protective effects of resveratrol on postmenopausal osteoporosis: Regulation of SIRT1-NF- $\kappa$ B signaling pathway. *Acta Biochim. Biophys. Sin.* **2014**, *46*, 1024–1033.
- (15) Zheng, C.-X.; Sui, B.-D.; Qiu, X.-Y.; Hu, C.-H.; Jin, Y. Mitochondrial Regulation of Stem Cells in Bone Homeostasis. *Trends Mol. Med.* **2020**, *26*, 89–104.
- (16) Indran, I. R.; Liang, R. L. Z.; Min, T. E.; Yong, E.-L. Preclinical studies and clinical evaluation of compounds from the genus *Epimedium* for osteoporosis and bone health. *Pharmacol. Ther.* **2016**, *162*, 188–205.
- (17) González-Osuna, L.; Sierra-Cristancho, A.; Rojas, C.; Cafferata, E. A.; Melgar-Rodríguez, S.; Cárdenas, A. M.; Vernal, R. Premature Senescence of T-cells Favors Bone Loss During Osteolytic Diseases. A New Concern in the Osteoimmunology Arena. *Aging Dis.* **2021**, *12*, 1150–1161.
- (18) Guo, Y.; Jia, X.; Cui, Y.; Song, Y.; Wang, S.; Geng, Y.; Li, R.; Gao, W.; Fu, D. Sirt3-mediated mitophagy regulates AGEs-induced BMSCs senescence and senile osteoporosis. *Redox Biol.* **2021**, *41*, 101915. Luo, H.; Gu, R.; Ouyang, H.; Wang, L.; Shi, S.; Ji, Y.; Bao, B.; Liao, G.; Xu, B. Cadmium exposure induces osteoporosis through cellular senescence, associated with activation of NF- $\kappa$ B pathway and mitochondrial dysfunction. *Environ. Pollut.* **2021**, *290*, 118043.
- (19) Fang, E. F.; Scheibye-Knudsen, M.; Brace, L. E.; Kassahun, H.; SenGupta, T.; Nilsen, H.; Mitchell, J. R.; Croteau, D. L.; Bohr, V. A. Defective mitophagy in XPA via PARP-1 hyperactivation and NAD<sup>+</sup>/SIRT1 reduction. *Cell* **2014**, *157*, 882–896.
- (20) Chandra, A.; Rajawat, J. Skeletal Aging and Osteoporosis: Mechanisms and Therapeutics. *Int. J. Mol. Sci.* **2021**, *22*, 3553.
- (21) Pan, J.-X.; Tang, F.; Xiong, F.; Xiong, L.; Zeng, P.; Wang, B.; Zhao, K.; Guo, H.; Shun, C.; Xia, W.-F.; Mei, L.; Xiong, W.-C. APP promotes osteoblast survival and bone formation by regulating mitochondrial function and preventing oxidative stress. *Cell Death Dis.* **2018**, *9*, 1077.
- (22) Ran, D.; Ma, Y.; Liu, W.; Luo, T.; Zheng, J.; Wang, D.; Song, R.; Zhao, H.; Zou, H.; Gu, J.; Yuan, Y.; Bian, J.; Liu, Z. TGF- $\beta$ -activated kinase 1 (TAK1) mediates cadmium-induced autophagy in osteoblasts via the AMPK/mTORC1/ULK1 pathway. *Toxicology* **2020**, *442*, 152538.
- (23) Domazetovic, V.; Marcucci, G.; Iantomasi, T.; Brandi, M. L.; Vincenzini, M. T. Oxidative stress in bone remodeling: Role of antioxidants. *Clin. Cases Miner. Bone Metab.* **2017**, *14* (2), 209–216.
- (24) Sánchez-Barceló, E. J.; Mediavilla, M. D.; Tan, D. X.; Reiter, R. J. Scientific basis for the potential use of melatonin in bone diseases: Osteoporosis and adolescent idiopathic scoliosis. *J. Osteoporosis* **2010**, *2010*, 830231.
- (25) Bianco, P.; Robey, P. G. Skeletal stem cells. *Development* **2015**, *142*, 1023–1027.
- (26) Pittenger, M. F.; Mackay, A. M.; Beck, S. C.; Jaiswal, R. K.; Douglas, R.; Mosca, J. D.; Moorman, M. A.; Simonetti, D. W.; Craig, S.; Marshak, D. R. Multilineage Potential of Adult Human Mesenchymal Stem Cells. *Science* **1999**, *284* (5411), 143–147.
- (27) Mackey, D. C.; Lui, L.-Y.; Cawthon, P. M.; Bauer, D. C.; Nevitt, M. C.; Cauley, J. A.; Hillier, T. A.; Lewis, C. E.; Barrett-Connor, E.; Cummings, S. R. High-trauma fractures and low bone mineral density in older women and men. *JAMA* **2007**, *298*, 2381–2388.
- (28) Åkesson, A.; Barregard, L.; Bergdahl, I. A.; Nordberg, G. F.; Nordberg, M.; Skerfving, S. Non-Renal Effects and the Risk Assessment of Environmental Cadmium Exposure. *Environ. Health Perspect.* **2014**, *122* (5), 431–438.
- (29) Tominaga, A.; Takaki, S.; Koyama, N.; Katoh, S.; Matsumoto, R.; Migita, M.; Hitoshi, Y.; Hosoya, Y.; Yamauchi, S.; Kanai, Y. Transgenic mice expressing a B cell growth and differentiation factor gene (interleukin 5) develop eosinophilia and autoantibody production. *J. Exp. Med.* **1991**, *173*, 429–437. Tägt, J.; Helte, E.; Donat-Vargas, C.; Larsson, S. C.; Michaëlsson, K.; Wolk, A.; Vahter, M.; Kippler, M.; Åkesson, A. Long-term cadmium exposure and fractures, cardiovascular disease, and mortality in a prospective cohort of women. *Environ. Int.* **2022**, *161*, 107114.
- (30) Hayman, A. R. Tartrate-resistant acid phosphatase (TRAP) and the osteoclast/immune cell dichotomy. *Autoimmunity* **2008**, *41* (3), 218–223. Vimalraj, S. Alkaline phosphatase: Structure, expression and its function in bone mineralization. *Gene* **2020**, *754*, 144855.
- (31) Bolamperti, S.; Villa, I.; Rubinacci, A. Bone remodeling: An operational process ensuring survival and bone mechanical competence. *Bone Res.* **2022**, *10*, 48. Yin, Z.; Zhu, W.; Wu, Q.; Zhang, Q.; Guo, S.; Liu, T.; Li, S.; Chen, X.; Peng, D.; Ouyang, Z. Glycyrrhizic acid suppresses osteoclast differentiation and postmenopausal osteoporosis by modulating the NF- $\kappa$ B, ERK, and JNK signaling pathways. *Eur. J. Pharmacol.* **2019**, *859*, 172550.
- (32) Yakout, S. M.; Alharbi, F.; Abdi, S.; Al-Daghri, N. M.; Al-Amro, A.; Khattak, M. N. K. Serum minerals (Ca, P, Co, Mn, Ni, Cd) and growth hormone (IGF-1 and IGF-2) levels in postmenopausal Saudi women with osteoporosis. *Medicine* **2020**, *99*, e20840. Alfvén, T.; Elinder, C.-G.; Carlsson, M. D.; Grubb, A.; Hellström, L.; Persson, B.; Pettersson, C.; Spång, G.; Schütz, A.; Järup, L. Low-Level Cadmium

Exposure and Osteoporosis. *J. Bone Miner. Res.* **2000**, *15* (8), 1579–1586.

(33) Martin, T. J.; Sims, N. A. RANKL/OPG; Critical role in bone physiology. *Rev. Endocr. Metab. Disord.* **2015**, *16* (2), 131–139.

(34) Collin-Osdoby, P.; Rothe, L.; Anderson, F.; Nelson, M.; Maloney, W.; Osdoby, P. Receptor activator of NF-kappa B and osteoprotegerin expression by human microvascular endothelial cells, regulation by inflammatory cytokines, and role in human osteoclastogenesis. *J. Biol. Chem.* **2001**, *276* (23), 20659–20672.

(35) Pearson, K. J.; Baur, J. A.; Lewis, K. N.; Peshkin, L.; Price, N. L.; Labinskyy, N.; Swindell, W. R.; Kamara, D.; Minor, R. K.; Perez, E.; Jamieson, H. A.; Zhang, Y.; Dunn, S. R.; Sharma, K.; Pleshko, N.; Woollett, L. A.; Csiszar, A.; Ikeno, Y.; Le Couteur, D.; Elliott, P. J.; Becker, K. G.; Navas, P.; Ingram, D. K.; Wolf, N. S.; Ungvari, Z.; Sinclair, D. A.; de Cabo, R. Resveratrol Delays Age-Related Deterioration and Mimics Transcriptional Aspects of Dietary Restriction without Extending Life Span. *Cell Metab.* **2008**, *8* (2), 157–168.

(36) Herranz, D.; Muñoz-Martin, M.; Cañamero, M.; Mulero, F.; Martinez-Pastor, B.; Fernandez-Capetillo, O.; Serrano, M. Sirt1 improves healthy ageing and protects from metabolic syndrome-associated cancer. *Nat. Commun.* **2010**, *1* (1), 3. Gomes, A. P.; Price, N. L.; Ling, A. J. Y.; Moslehi, J. J.; Montgomery, M. K.; Rajman, L.; White, J. P.; Teodoro, J. S.; Wrann, C. D.; Hubbard, B. P.; Mercken, E. M.; Palmeira, C. M.; de Cabo, R.; Rolo, A. P.; Turner, N.; Bell, E. L.; Sinclair, D. A. Declining NAD<sup>+</sup> Induces a Pseudohypoxic State Disrupting Nuclear-Mitochondrial Communication during Aging. *Cell* **2013**, *155* (7), 1624–1638.

(37) Lemieux, M. E.; Yang, X.; Jardine, K.; He, X.; Jacobsen, K. X.; Staines, W. A.; Harper, M. E.; McBurney, M. W. The Sirt1 deacetylase modulates the insulin-like growth factor signaling pathway in mammals. *Mech. Ageing Dev.* **2005**, *126* (10), 1097–1105.

(38) Cheng, H.-L.; Mostoslavsky, R.; Saito, S.; Manis, J. P.; Gu, Y.; Patel, P.; Bronson, R.; Appella, E.; Alt, F. W.; Chua, K. F. Developmental defects and p53 hyperacetylation in Sir2 homolog (SIRT1)-deficient mice. *Proc. Natl. Acad. Sci. U. S. A.* **2003**, *100*, 10794–10799.

(39) Zainabadi, K. Drugs targeting SIRT1, a new generation of therapeutics for osteoporosis and other bone related disorders? *Pharmacol. Res.* **2019**, *143*, 97–105.

(40) Zainabadi, K.; Liu, C. J.; Caldwell, A. L. M.; Guarente, L. SIRT1 is a positive regulator of in vivo bone mass and a therapeutic target for osteoporosis. *PLoS One* **2017**, *12*, e0185236. Simic, P.; Zainabadi, K.; Bell, E.; Sykes, D. B.; Saez, B.; Lotinun, S.; Baron, R.; Scadden, D.; Schipani, E.; Guarente, L. SIRT1 regulates differentiation of mesenchymal stem cells by deacetylating  $\beta$ -catenin. *EMBO Mol. Med.* **2013**, *5* (3), 430–440.

(41) Sadeghi, H.; Azarmehr, N.; Razmkhah, F.; Sadeghi, H.; Danaei, N.; Omidifar, N.; Vakilpour, H.; Pourghadamyari, H.; Doustimotlagh, A. H. The hydroalcoholic extract of watercress attenuates protein oxidation, oxidative stress, and liver damage after bile duct ligation in rats. *J. Cell Biochem.* **2019**, *120* (9), 14875–14884. Verstraeten, S. V.; Aimo, L.; Oteiza, P. I. Aluminium and lead: Molecular mechanisms of brain toxicity. *Arch. Toxicol.* **2008**, *82* (11), 789–802.

(42) Vaziri, H.; Dessari, S. K.; Eaton, E. N.; Imai, S.-I.; Frye, R. A.; Pandita, T. K.; Guarente, L.; Weinberg, R. A. hSIR2/SIRT1 Functions as an NAD-Dependent p53 Deacetylase. *Cell* **2001**, *107* (2), 149–159.

(43) Appella, E.; Anderson, C. W. Post-translational modifications and activation of p53 by genotoxic stresses. *Eur. J. Biochem.* **2001**, *268* (10), 2764–2772. Brooks, C. L.; Gu, W. Ubiquitination, phosphorylation and acetylation: The molecular basis for p53 regulation. *Curr. Opin. Cell Biol.* **2003**, *15* (2), 164–171.

(44) Schwer, B.; Verdin, E. Conserved Metabolic Regulatory Functions of Sirtuins. *Cell Metabolism* **2008**, *7* (2), 104–112. Haigis, M. C.; Guarente, L. P. Mammalian sirtuins—emerging roles in physiology, aging, and calorie restriction. *Genes Dev.* **2006**, *20* (21), 2913–2921.

(45) Anderson, R. M.; Barger, J. L.; Edwards, M. G.; Braun, K. H.; O'Connor, C. E.; Prolla, T. A.; Weindruch, R. Dynamic regulation of PGC-1 $\alpha$  localization and turnover implicates mitochondrial adaptation in calorie restriction and the stress response. *Aging Cell* **2008**, *7* (1), 101–111.

(46) Arany, Z.; He, H.; Lin, J.; Hoyer, K.; Handschin, C.; Toka, O.; Ahmad, F.; Matsui, T.; Chin, S.; Wu, P.-H.; Rybkin, I. I.; Shelton, J. M.; Manieri, M.; Cinti, S.; Schoen, F. J.; Bassel-Duby, R.; Rosenzweig, A.; Ingwall, J. S.; Spiegelman, B. M. Transcriptional coactivator PGC-1 $\alpha$  controls the energy state and contractile function of cardiac muscle. *Cell Metab.* **2005**, *1* (4), 259–271. St-Pierre, J.; Lin, J.; Krauss, S.; Tarr, P. T.; Yang, R.; Newgard, C. B.; Spiegelman, B. M. Bioenergetic Analysis of Peroxisome Proliferator-activated Receptor  $\gamma$  Coactivators 1 $\alpha$  and 1 $\beta$  (PGC-1 $\alpha$  and PGC-1 $\beta$ ) in Muscle Cells\*. *J. Biol. Chem.* **2003**, *278* (29), 26597–26603.

(47) Chang, Y.-C.; Liu, F.-P.; Ma, X.; Li, M.-M.; Li, R.; Li, C.-W.; Shi, C.-X.; He, J.-S.; Li, Z.; Lin, Y.-X.; Zhao, C.-W.; Han, Q.; Zhao, Y.-L.; Wang, D.-N.; Liu, J.-L. Glutathione S-transferase A1—A sensitive marker of alcoholic injury on primary hepatocytes. *Hum. Exp. Toxicol.* **2017**, *36* (4), 386–394.

(48) Denu, J. M. The Sir2 family of protein deacetylases. *Curr. Opin. Chem. Biol.* **2005**, *9* (5), 431–440.

(49) Winter, J. M.; Yadav, T.; Rutter, J. Stressed to death: Mitochondrial stress responses connect respiration and apoptosis in cancer. *Mol. Cell* **2022**, *82*, 3321.

(50) Kelly, D. P.; Scarpulla, R. C. Transcriptional regulatory circuits controlling mitochondrial biogenesis and function. *Genes Dev.* **2004**, *18*, 357–368.

## Recommended by ACS

### Effect of the Amylose Nanoscale Polymerization Index on the Digestion Kinetics and Mechanism of Recombinant Chinese Seedless Breadfruit Starch Triadic Complexes

Bo Li, Lehe Tan, *et al.*

APRIL 06, 2023

JOURNAL OF AGRICULTURAL AND FOOD CHEMISTRY

READ 

### Heat Stress-Induced Intestinal Barrier Impairment: Current Insights into the Aspects of Oxidative Stress and Endoplasmic Reticulum Stress

Zhining Tang, Yun Ji, *et al.*

APRIL 03, 2023

JOURNAL OF AGRICULTURAL AND FOOD CHEMISTRY

READ 

### Nanoencapsulation Motivates the High Inhibitive Ability of Fucoxanthin on H<sub>2</sub>O<sub>2</sub>-Induced Human Hepatocyte Cell Line (L02) Apoptosis via Regulating Lipid Metabolism Homeos...

Chunyan Wang, Hang Qi, *et al.*

APRIL 07, 2023

JOURNAL OF AGRICULTURAL AND FOOD CHEMISTRY

READ 

### Stacks of Equidistant 5,6-Dichloro-2,3-dicyanosemiquinone (DDQ) Radicals under Variable-Temperature and High-Pressure Conditions

Petra Stanić, Krešimir Molčanov, *et al.*

APRIL 13, 2023

CRYSTAL GROWTH & DESIGN

READ 

Get More Suggestions >